High-pressure phase transformations in liquids and amorphous solids

2003 J. Phys.: Condens. Matter 15 6059

(http://iopscience.iop.org/0953-8984/15/36/301)

INSTITUTE OF PHYSICS PUBLISHING JOURNAL OF PHYSICS: CONDENSED MATTER

J. Phys.: Condens. Matter **15** (2003) 6059–6084 PII: S0953-8984(03)56645-0

High-pressure phase transformations in liquids and amorphous solids

V V Brazhkin and A G Lyapin

Institute for High Pressure Physics, Russian Academy of Sciences, Troitsk, Moscow region 142190, Russia

Received 25 November 2002
Published 29 August 2003
Online at stacks.iop.org/JPhysCM/15/6059

Abstract

We outline the current state of experimental study and basic ideas for describing phase transitions in topologically disordered condensed matter, such as liquids and amorphous solids. Reviewing briefly the study of molten elementary substances under pressure, we pay primary attention to the results for liquid Se, S, and P and also to those substances that have not been represented in previous publications, mainly the liquid oxides B_2O_3 and GeO_2. The experimental data reveal the possibility of rather sharp transformations in relatively simple liquids that are smoothed at high temperatures. Comparing the transitions in amorphous solids and in liquids, one should emphasize the metastable and non-ergodic nature of amorphous substances and the existence of static local atomic stresses fluctuating in thermally frozen amorphous networks. In particular, the kinetic study of amorphous–amorphous transformations (AATs) in SiO_2 and GeO_2 glasses and amorphous H_2O ice under pressure highlights a number of anomalous features that distinguish the AATs from ordinary first-order transitions and from transformations in liquids. The recent *in situ* study of the volume changes in glassy silica a-SiO_2 upon compression at high temperatures provides a new conclusion as regards the existence of two pressure-induced AATs in a-SiO_2 with different microscopic mechanisms of structural rearrangements. We also perform the analysis of two possible kinetic scenarios for AATs, including sharp and diffuse transitions. The key relation determining the transformation scenario is the relationship between the radius of structural correlations in amorphous solid and the size of the critical nucleus of the growing disordered modification. The comparative analysis emphasizes the main difference between the transformations in liquids and amorphous solids that consists in the fact that the transitions in liquids are mainly determined by thermodynamic relationships, whereas the transitions in amorphous solids take place far away from equilibrium and are governed by the corresponding kinetics.

1. Introduction

The phase transitions induced by changes in external parameters and accompanied by drastic changes in the properties and structure of substances are prevalent in nature. The theory of phase transitions with discontinuous changes of density and entropy, accepted in thermodynamics as the first-order transitions, is of special interest when there is a considerable rearrangement of the atomic packing in a substance, accompanied by changes in the short- and/or long-range-order structure. Whereas the first-order phase transitions between different aggregate states or crystalline phases have been studied, both experimentally and theoretically, fairly thoroughly, the very possibility of phase transitions between different states of disordered substances, such as liquids and amorphous solids, is still questionable. If drastic changes in the properties and structure of disordered phases are possible, it is necessary to determine clearly the nature and driving forces of these transformations, and to introduce correctly the order parameter for these transitions.

Pressure and temperature variations must induce changes in the properties and structure (mainly the short-range-order structure) of a liquid and the electron states of atoms in a liquid [1]. Liquid crystals [2] are well-known examples in which different liquid modifications do exist, and first-order phase transitions between liquid states become possible. There exists long-range translation order, and it is easy to introduce the order parameter for phase transitions in this case. The introduction of the order parameter for possible liquid–liquid phase transitions in relatively simple isotropic liquids is much more difficult.

Anomalous changes of properties and short-range-order structure induced by variation of external parameters have already been detected for tens of melts [1, 3]. Interpreted as transformations, these anomalies are diffuse enough in most cases. However, there are indications that sharp transitions under pressure, formally similar to first-order phase transitions, exist for liquid phosphorus [4], selenium [5], sulfur [6, 7], supercooled water [8], and possibly liquid carbon [9, 10]. Nevertheless, the sharpness of transitions in these liquids remains open to question, and the change of basic thermodynamic and kinetic properties of these melts is still not cleared up.

The description of phase transitions in amorphous solids is complicated by their metastability, non-ergodicity, and, as a consequence, the possibility of irreversible relaxation of their properties and structure. It is topical to introduce specific criteria for the existence of a phase transition between metastable states. In particular, all activation energy barriers corresponding to the transition between two metastable states should be lower than those for the rearrangement of both the metastable states involved to more stable phases. Otherwise, the 'equilibrium' transition between metastable modifications (e.g., between two amorphous phases) is inaccessible at all, and the real transformation should follow a quite different scenario than that corresponding to thermodynamic relations between the Gibbs free energies of metastable phases.

On the other hand, one can note that phase transitions in crystalline solids occur through the nucleation and diffusive growth of a new phase (diffusive transitions) or as coherent atomic rearrangement in large domains of the lattice (martensitic transitions). Neither of the two opportunities can be realized in the case of transformations between amorphous phases. Long-range diffusion is frozen in the temperature range of existence of metastable amorphous phases, whereas the coherent motion of atoms is impossible in a geometrically disordered system.

The existence of reversible transformations between amorphous modifications (polyamorphism) involving changes in the local order structure and density has been firmly established by different experimental techniques for SiO_2 and GeO_2 oxide glasses [11–17] and for amorphous H_2O ice [18–20]. Moreover, there is experimental evidence for transitions under

pressure in other amorphous materials, for example, between the amorphous modifications of carbon [21, 22] and in the borate [23] and aluminate [24] glasses. A great number of experiments show a wide range of amorphous–amorphous transformations (AATs) in silica and germania glasses under pressure [11–17, 25–29]. Meanwhile the sharp transformation between the low-density (lda) and high-density (hda) forms of amorphous ice is considered now as a first-order transition [8, 18–20]. The mechanism of AAT in ice is of specific relevance for our understanding of puzzling water properties and for discussing a possible first-order liquid–liquid phase transition in water with the boundary line terminating at the second critical point in the supercooled region [8].

It is important that transformation in the amorphous state occurs far from thermodynamic equilibrium, which means that kinetic aspects of the transformation are of special interest for understanding the transformation mechanism. At the same time, the kinetics of transitions in the amorphous state and elastic properties of amorphous phases under pressure have been scarcely studied previously.

Here we consider liquids and amorphous phases as two different states of matter. Meanwhile the glass or amorphous phase can be regarded, in many respects, as a 'frozen' analogue of the corresponding liquid. In this respect, the study of interrelations of transformations between relevant liquid and amorphous phases is of great interest. However, there are virtually no substances for which it would be possible to study experimentally the transitions between pairs of stable liquids, supercooled liquid states, and corresponding amorphous phases. The amorphous phases of Se, S, P, Te, and I easily crystallize under pressure at room temperature. At the same time, the liquid phases of SiO_2 and GeO_2 are difficult to study experimentally due to their high temperature of melting. Transitions in strongly supercooled liquid states are mainly a subject for computer experiments, e.g., for supercooled H_2O water (see [8] and reference therein).

Here we review the results of our scientific group on the subjects discussed, consider other relevant data, and try to highlight an interrelation between transformations in the liquid and amorphous states, as well as distinctions and specific features of these transformations. The paper is structured as follows. In section 2 we briefly describe the experimental techniques involved in our experiments and their specificities with respect to liquid and solid matter. The results of experimental study of the transitions in the melts of a number of elements and some oxides are presented in section 3. The kinetic study of the structural transformation in a-SiO_2 and a-GeO_2, as well as the study of elastic changes and kinetic relaxations during lda–hda transformations in H_2O ice (section 4), clarify in many respects the specific aspects of the polyamorphism in these substances. Very recent results on the transformations in a-SiO_2 at high temperatures under pressure are also discussed in this section. In comparing the data on the transformations in melts and amorphous solids, the importance of existing 'frozen' stresses in the latter is noteworthy and discussed in section 5. We also consider in section 5 the two possible scenarios of transformations in disordered matter, sharp and diffuse, providing for the first time the criteria controlling the realization of the particular scenario in a specific amorphous substance.

2. Experimental techniques

2.1. Liquid matter

Study of highly compressed melts is a rather complicated experimental task involving the simultaneous application of high pressures and high temperatures. Moreover, many melts are extremely chemically active and thus require special containers and conducting leads. We used

various modifications of the 'toroid' chamber [30] that allow us to generate pressures up to 0.3–13 GPa and temperatures up to 77–2300 K. High temperatures were produced by resistive heating. The conductivity of melts was measured by the four-probe method using carbon fibres as conducting leads, or was estimated from the voltage–current ratio. Heat anomalies were registered by differential thermal analysis (DTA). Volume anomalies were registered and estimated from the data from thermobaric analysis (TBA), the original technique based on 'thermo-emf' measurements in the vicinity of the sample [31, 32]. Pressure anomalies were detected using simultaneous readings from two thermocouples with different pressure coefficients of the thermo-emf, for example, the chromel–alumel and Pt–Pt + Rh ones. This technique is contact-free and allows us to record the volume anomalies $\Delta V/V > 0.5\%$ [31, 32]. The absolute precision of this method is not too high, but it ensures volume measurements at high temperatures up to 1700 K.

For several melts (Se, S, P, B_2O_3), studies of the supercooling kinetics and the pressure dependence of the grain size for samples crystallized by rapid quenching from the melt under pressure (at the cooling rates 10^{-1}–10^3 K s^{-1}) were performed. From these data one can estimate the pressure dependences of the melt viscosity and surface tension [33, 34].

2.2. Amorphous substances

Precise volumetric studies of oxide glasses were accomplished using the strain gauge technique. All details concerning the preparation of gauges and high-pressure assembly, as well as high-pressure experiments, are presented elsewhere [35]. The absolute accuracy of volume measurements by the strain gauge technique was about 0.3%. At the same time, the relative sensitivity of this method, which is particularly critical for time-dependent relaxation measurements, is much better, $\Delta V/V \sim 10^{-5}$ [35]. The modification of the strain gauge technique for high temperatures [36] provided the possibility to study transformations in a-SiO_2 at high-pressure–high-temperature conditions. The density of glassy silica was measured *in situ* at high pressures up to 9 GPa and temperatures up to 730 K at both compression and decompression.

The density and elastic properties of H_2O ice were measured in the pressure range up to 2.0 GPa and temperature range 77–300 K by the ultrasonic technique using a high-pressure device of the cylinder–piston type [37]. The measurements were performed by the pulsed ultrasonic method [38] using x-cut and y-cut quartz plates as piezoelectric sensors with a carrier frequency of 5 MHz. The bulk, B, and shear, G, elastic moduli were calculated from the values of transverse, V_t, and longitudinal, V_l, wave velocities using the standard equations for the isotropic elastic medium.

3. Liquids

3.1. Transformations in molten elementary substances

It has been established that several elementary liquids (Se, S, Bi, P, I_2, Sn, and Sb) and molten compounds (As_2Se_3, As_2S_3, and Mg_3Bi_2) undergo pressure-induced transitions in rather narrow pressure–temperature intervals, similarly to the first-order phase transitions [1, 39]. These transformations are accompanied by volume and heat anomalies, as well as by sharp changes in the viscosity and resistivity of melts. With the temperature increase, the anomalies become diffuse and cannot be recognized at the temperatures $T \approx (1.3\text{–}1.5)T_m$, where T_m is the melting temperature. In such substances as Se, S, Te, P, I_2, As_2Se_3, As_2S_3, and Mg_3Bi_2, the semiconductor-to-metal transition is observed under compression; the pressure

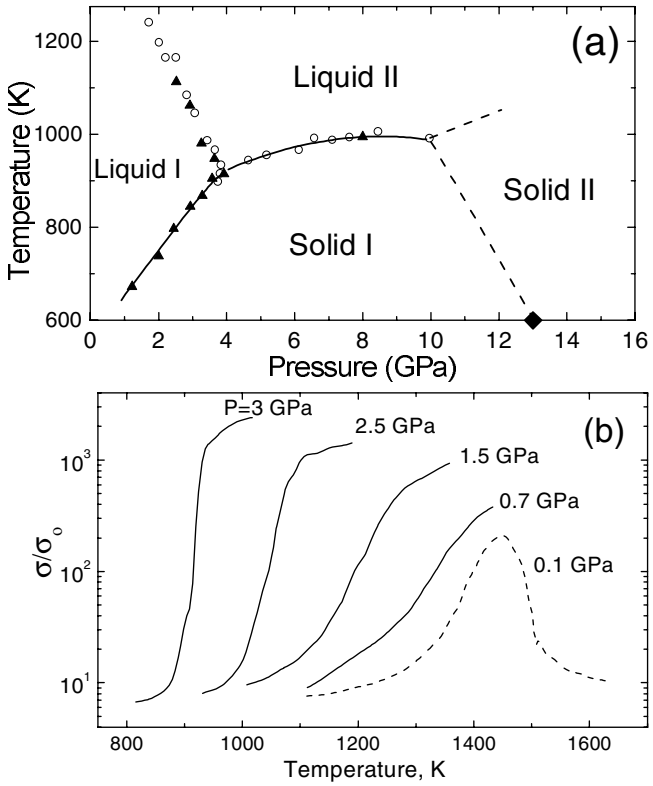

Figure 1. (a) The pressure–temperature phase diagram of crystalline and liquid Se, according to [5]. (b) Temperature dependences of the relative conductivities σ/σ_0 of Se melts at various pressures. The curve for $P = 0.1$ GPa is taken from [65].

of metallization for liquids is significantly lower than that for the corresponding crystals. The most important results on the transformations in liquids discussed were published in the original papers [1, 5, 6, 40–47] and summarized in the previous review [1]. Here we mainly discuss the results that have not been adequately considered previously or were not reported at all.

Selenium was the first elementary substance in which the volume and heat anomalies were observed in the molten state (figure 1(a)). These anomalies were accompanied by the metallization of the liquid (figure 1(b)) [5]. Near the melting curve this transformation takes place at the pressure ≈4 GPa with a transition width less than 0.3 GPa, or at 30 K, when temperature is changed. The conductivity increases by two orders of magnitude from ≈10 to $10^3\ \Omega^{-1}\ \mathrm{cm}^{-1}$. With the temperature growth, the transition becomes diffuse and terminates near the critical region at $P \approx 1$ GPa and $T \approx 1300$ K. The volume anomaly was estimated to be equal to ≈5%, and at $P \approx 4$ GPa the melting curve slope diminishes approximately by half.

The study of crystallization of the selenium melt under high pressure and rapid cooling is of great interest [43]. At $P < 1$ GPa the rapidly quenched ($\mathrm{d}T/\mathrm{d}t > 10^2\ \mathrm{K\ s}^{-1}$) selenium melt transforms to glass. At higher pressures, molten Se crystallizes during cooling, the grain size increasing with the quenching pressure growth. At $P \approx 4$ GPa the grain size is maximum (≈200–300 μm), and further pressure increase leads to diminishing of the grain size (figure 2(a)). The supercooling of molten Se is, in contrast, minimum at a pressure equal

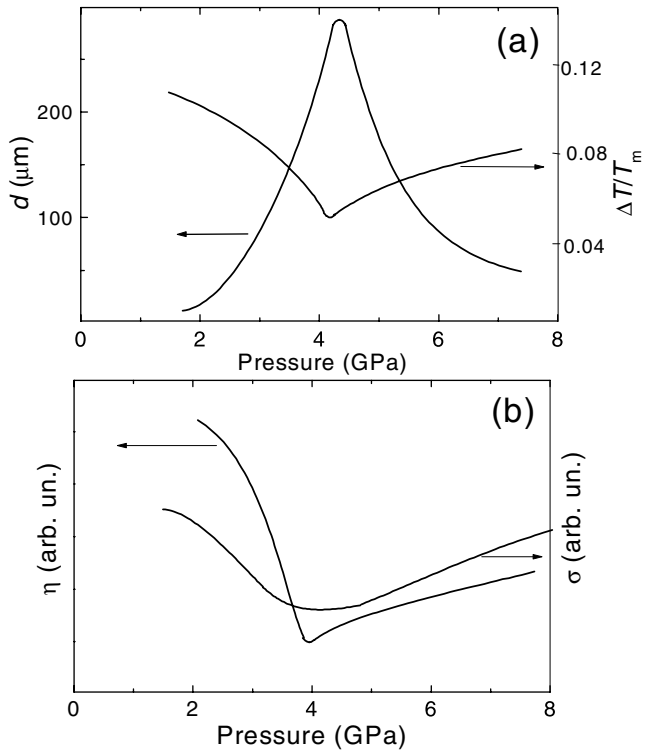

Figure 2. (a) Pressure dependences of the undercooling ΔT, normalized to the melting temperature T_m, of liquid Se for rapid quenching from the melt, and the average grain size d in crystallized samples. (b) Estimated pressure dependences of the viscosity ν and surface tension σ for the Se melt. All dependences are obtained by interpolation of experimental points [43].

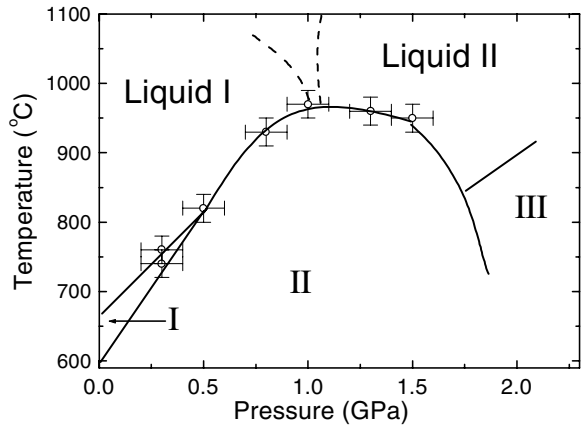

Figure 3. The pressure–temperature phase diagram of phosphorus [39].

to 4 GPa (figure 2(a)). The data obtained reveal a significant viscosity decrease of the selenium melt before metallization, and a change of the viscosity pressure coefficient after the transition (figure 2(b)) [43].

Sulfur is one of a few elementary substances in which property anomalies and possible phase transitions in the molten state have been known of for a long time [48]. The diversity of molten states at low pressures is due to a complicated molecular structure of molten S, comprising chains, globules, etc. Our study has revealed the existence of at least two lines of phase transitions in liquid sulfur at the pressures $P > 1$ GPa [6]. In the vicinity of the melting line, these transitions occur at $P \approx 8$ and 12 GPa. The first transition is accompanied by a significant volume anomaly without metallization, whereas the second one taking place at higher pressures is analogous to the metallization of liquid Se and is accompanied by increase of the conductivity by 1–2 orders of magnitude. As the temperature increases, the transitions become diffuse near the critical regions similarly to the transition in liquid Se. The very recent structural study of liquid S [7] also points to sharp structural changes in the melt in definite pressure–temperature regions.

Like sulfur, liquid phosphorus has an intricate molecular structure. The P_4 tetrahedra are known to be its structural units [49]. We have established that the metallization of liquid phosphorus was observed at the pressure $P \approx 1$ GPa [1] (figure 3). At $P \approx 0.7$ GPa the conductivity of liquid P is $\sigma < 10\ \Omega^{-1}\ \mathrm{cm}^{-1}$, whereas at $P > 1.2$ GPa, $\sigma \approx 10^3\ \Omega^{-1}\ \mathrm{cm}^{-1}$. The observation of the semiconductor-to-metal transition in liquid P has been confirmed recently by the computer simulation work [50]. Like in Se, the metallization of molten P leads to a significant decrease of its viscosity. The maximum grain size of crystallized black phosphorus, $\approx$500 μm, is attained under the pressure $P \approx 1.1$ GPa, thus revealing an extremely low viscosity of the melt at this pressure. The data on liquid phosphorus crystallization along with indirect indications of its low viscosity are in contradiction with the polymerized state of liquid P under high pressure suggested by Katayama *et al* [4]. A zero or slightly negative slope of the melting line of phosphorus at $P > 1.2$ GPa proves that the metallic melt of P has a density at least not lower than the density of black crystalline phosphorus. Hence, the melt of phosphorus has a rather high coordination number at these pressures.

3.2. Liquid SiO_2

As mentioned above, the experimental properties of the SiO_2 melt under high pressure have practically not been studied due to the very high melting temperatures and related experimental difficulties. Nevertheless, it follows from the theoretical calculations [51, 52] that smooth change of the short-range-order structure takes place in the SiO_2 melt within the range 5–15 GPa. This change is accompanied by a corresponding horizontal flattening of the pressure dependence of the melting temperature [53, 54] and by an anomalous reduction of viscosity with the pressure growth [55, 56]. In addition, an anomalous densification of glasses obtained from the melt is observed in the range 2–4 GPa [53]. These data will be discussed in section 5, where they are compared with the results relating to the transformation in a-SiO_2 under pressure.

3.3. Liquid GeO_2

Germanium dioxide is the closest structural analogue of silica. Two stable crystalline phases, quartz-type and rutile-type, are present in its phase diagram at pressures up to 20 GPa, and the rutile-type modification is stable at normal conditions [57]. The experimental properties of the GeO_2 melt have been scantily studied before. The main obstacle to studying liquid GeO_2 is the easy decomposition of GeO_2 into elementary germanium and oxygen under high pressures and temperatures [58]. As far as we know, there exists only one work [59] in which the melting curve of GeO_2 was studied up to pressures of 2 GPa, but there is also a work [60] where a strong fivefold decrease of viscosity of the GeO_2 melt (also indicative of transformation in the short-range-order structure) was observed under isothermal compression up to 0.95 GPa.

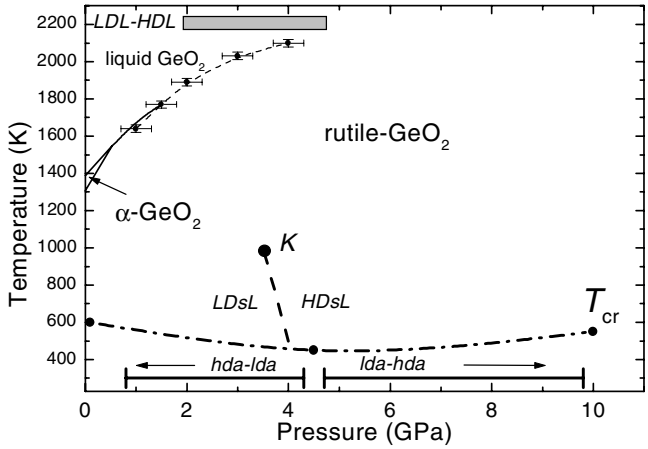

Figure 4. The pressure–temperature phase diagram of GeO_2. The points on the melting curve and the line of crystallization (T_{cr}), as well as intervals of AATs (horizontal bars) between low-density and high-density amorphous phases (lda and hda), are obtained experimentally. The grey bar shows the supposed pressure interval for transformation between low-density and high-density liquids (LDL–HDL). The hypothetical transition between supercooled liquids (LDsL and HDsL) with the supposed line of the first-order phase transition (dashed curve) terminating at the critical point '*K*' is also illustrated.

We studied the high-temperature part of the phase diagram of GeO_2 and the melting curve up to pressure 4 GPa (figure 4). The experiments were performed in an especially designed closed ampoule made from Ta, in order to avoid the decomposition of GeO_2. The horizontal flattening of the melting curve at $P \sim 2$–4 GPa indicates a considerable densification of the melt, related possibly to a diffuse transformation from the quartz-like liquid to the rutile-like one. This hypothetical transformation in the GeO_2 melt will be discussed in section 5, when we will compare the behaviours of liquid- and glass-like GeO_2.

3.4. Liquid B_2O_3

The B_2O_3 compound, owing to its rather low temperature of melting ($T_m \approx 800$ K at room pressure) and glass transition ($T_g \approx 500$ K) [61], seems at first sight a good object for study and for which to compare the transitions in the liquid and glass states. However, x-ray diffraction study of B_2O_3 under pressure is quite difficult due to the small scattering factor of the substance. As far as the melting curve and phase diagram of B_2O_3 are concerned, a few attempts at their study were undertaken about 40 years ago [23, 62]. The liquid state of B_2O_3 under pressure has not been studied previously. The effect of densification of glasses after pressure treatment, both at room and at high temperatures, was known for glass B_2O_3 [23]. It is also known that slow cooling ($T \sim 10^{-2}$ K s^{-1}) of the B_2O_3 melt at $P \sim 1$ GPa results in the growth of large crystals, whereas, at normal pressure, at virtually any cooling rate ($T > 10^{-5}$ K s^{-1}) the glass is formed.

In the course of our investigations, we studied the phase diagram of B_2O_3 within the pressure range up to 8 GPa (figure 5(a)) using the DTA and TBA methods, as well as the results of quenching experiments. It is necessary to note a strong change in the melting curve within the range 1.5–2.5 GPa. A substantial anomaly in the glass density for B_2O_3 glass samples prepared by quenching is also detected for the same range of preparation pressures (figure 5(b)). One could suggest that a transformation, accompanied by changes of the volume and structure,

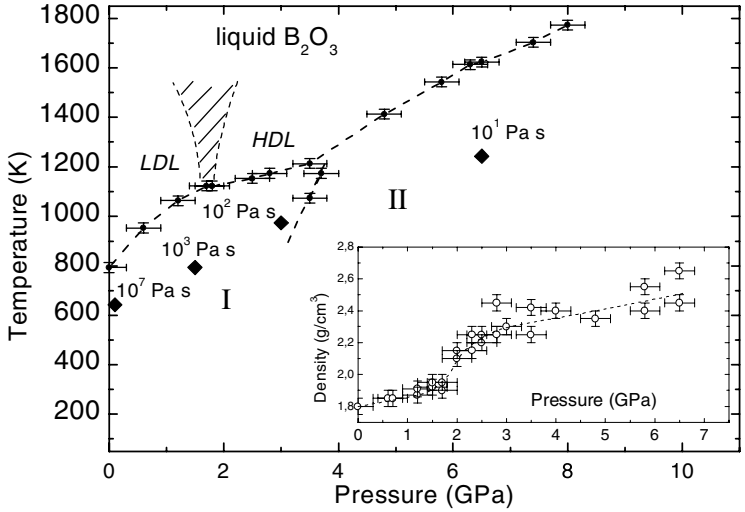

Figure 5. The experimentally studied pressure–temperature phase diagram of B_2O_3, including melting points and points of transition between crystalline modifications (I and II). Diamonds show points, where the viscosity of the undercooled melt was estimated from quenching experiments. These points are labelled with the corresponding values of viscosity. The room pressure density versus the pressure of quenching dependence for the pressure-synthesized glass samples, in the inset, allows one to suppose the existence of a transformation between low-density and high-density liquids (LDL and HDL), also illustrated in the diagram.

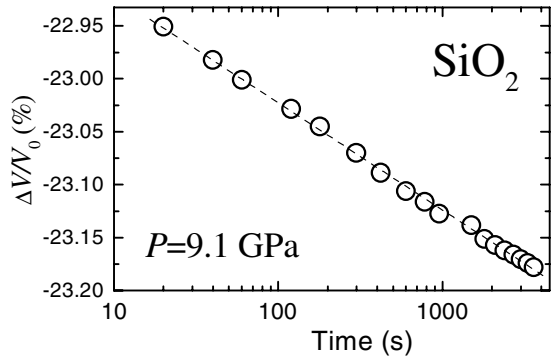

Figure 6. The temporal dependence of the relative volume for a-SiO_2 under pressure [68].

takes place in the liquid B_2O_3 in this relatively narrow pressure range. Preliminary study of the specific volume of liquid B_2O_3 by the TBA method in fact indicates an anomaly of the melt density at pressures of 2–2.5 GPa. In turn, at higher pressures there exists an additional growth of the density of quenched glasses up to the values of 2.5–2.6 g cm^{-3} (figure 5(b)). However, the possibility of a second transformation in the B_2O_3 melt, as well as the structural genesis of the first transformation at $P \sim 2$ GPa, requires additional studies.

In addition, we carried out experiments on the cooling of the B_2O_3 melt under pressure at various rates, which has provided the possibility of evaluating the pressure dependence of the melt viscosity. The viscosity of the liquid at a sufficient accuracy is inversely proportional to the critical rate of cooling, corresponding to the change between vitrification and crystallization regimes during cooling [44, 63]. In this case, the melt viscosity is evaluated near the

temperature of the maximum crystallization rate, which is $(0.75–0.8)T_m$ [61, 64]. The critical cooling rate for the glass formation at $P \sim 1, 5$ GPa was measured to be equal to 1 K s^{-1}, at 3 GPa to 10 K s^{-1}, and at 6 GPa to 10^2 K s^{-1}. The evaluated pressure dependence of the melt viscosity is illustrated in figure 5.

3.5. Summary remark

Summarizing, it may be inferred that sufficiently sharp and relatively narrow transformations are possible both in the melts of elementary substances and in the melts of oxides under pressure. These transformations are accompanied by changes in the volume and short-range-order structure, as well as by anomalies in the kinetic properties. The degree of sharpness for specific transformations, the transition mechanisms, and the types of short-range-order structure for the corresponding liquid phases require further study.

4. Amorphous solids

4.1. SiO_2 and GeO_2 glasses

In spite of great experimental efforts [8, 11–20, 65–70] the nature of the phase transformations in topologically disordered systems such as amorphous solids has not been adequately studied as yet. Silica is the most important glass-forming material. Vitreous germania a-GeO_2 is an excellent chemical and structural analogue of silica glass. The strain gauge technique study of the pressure and temporal dependences of density in silica and germania glasses under pressures up to 9.0 GPa [68, 70] provided quite new fundamental information on the mechanism of transformation in these glasses.

In particular, after pressurization, the sample of a-SiO_2 was kept at $P = 9.0$ GPa for one hour. There was detected an irreversible densification of the sample, that can be described by the logarithmic law $\Delta V/V \sim \log(t)$, to a high accuracy (figure 6). The density versus pressure curve for decompression is shifted toward higher densities.

Two kinds of experiments were carried out for a-GeO_2 under pressure. In the first experiment, the glass sample was pressurized and depressurized under a continuous pressure variation ($\mathrm{d}P/\mathrm{d}t \sim 0.1$ GPa min^{-1}), and in the second experiment the pressure increase was interrupted by the volume versus time measurements at fixed pressures for ~100 min or longer. The direct (up to 9 GPa) and reverse equations of state are presented in figure 7(a). The volume versus pressure curves for the continuous and intermittent pressure increase experiments are very close to each other (figure 7(b)). The important feature for the experiments of the second type is that the pressure increase between the breaks for time measurements results in return of the $V(P)$ curve to the dependence observed for a continuous pressure increase (figure 7(b)). From the compressibility curve, the reverse transformation begins at $P \approx 4$ GPa, where we directly found an irreversible volume change with time.

The results of volume versus time measurements are shown in figure 8. Direct evidence of time-dependent irreversible relaxation was found at $P = 3$ GPa, in the region of divergence between the quasi-static and ultrasonic (or Brillouin) equations of state. However, the inelastic behaviour seems to appear in a-GeO_2 even below this, at $P \approx 2$ GPa, where the relaxed compressibility starts to increase. The time dependence of the volume decrease (figure 8) is described by the curves, which are nearly linear for a sufficiently long time interval in the $\Delta V/V$ versus $\log(t)$ coordinates.

The following four major features of the AAT in a-GeO_2 and a-SiO_2 stand out.

(i) The anomaly corresponding to the coordination compaction of the amorphous GeO_2 network was recorded over a broad pressure range.

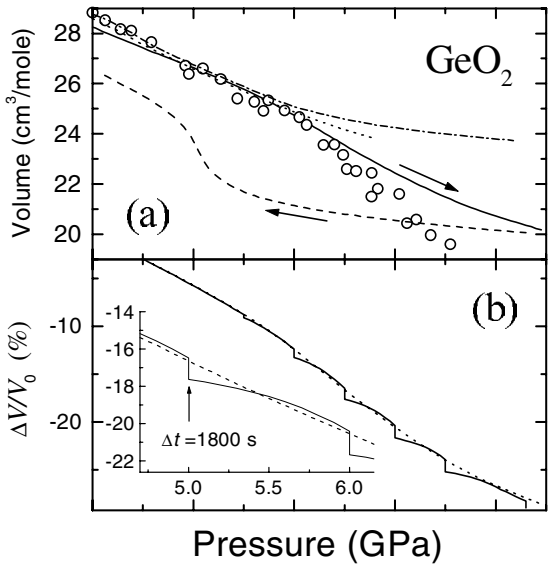

Figure 7. (a) The equation of state of a-GeO_2 [68] in comparison with the volumetric data of Smith *et al* [17] (circles) and the Brillouin [29] (dashed and dotted) and ultrasonic [72] (dotted) equations of state. (b) Volume change in the experiment with a continuous variation of the pressure (dashed line) compared with that in the experiment with the intermittent compression (solid curve) [68].

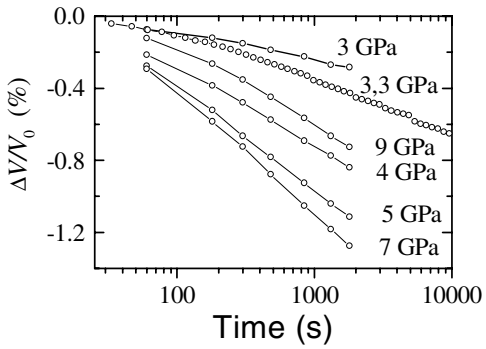

Figure 8. Temporal dependences of the relative volume for a-GeO_2 at different pressures [68].

(ii) For a fixed pressure, the logarithmic (or close to logarithmic) change of volume with time is observed in the transition range (figures 6 and 8). The typical amplitude of the relaxation depends only slightly on the pressure.

(iii) Upon prolonged exposure to a fixed pressure, in response to the relaxation, the quasi-static compressibility decreases sharply to the values resulting from ultrasonic and Brillouin experiments at these pressures [29, 71, 72]. Upon further pressure increase, the compressibility increases again, i.e. the amorphous network 'forgets' about the preceding relaxation.

(iv) A 'negative' hysteresis is observed for the coordination transition in a-GeO_2, i.e. the reverse transformation starts at $P \approx 4$ GPa in the pressure range of the direct transition, the onset of which was recorded at $P \approx 3$ GPa.

The above-listed features of the transformation in a-GeO_2 and the relaxation in a-SiO_2 at the coordination transition onset differ radically from the features of conventional first-order phase transitions. In fact, the logarithmic kinetics is inherent in various disordered systems [73–76]. The logarithmic relaxation is associated with the existence of a continuous spectrum of relaxation times [77]. As far as the structural transformations are concerned, this means a wide hierarchy of structural processes with the uniform distribution of energy barriers.

The very recent study [36] of density variation for glassy silica at elevated temperatures has made it possible to clarify the pattern of the transformation in a-SiO_2. The curves for the relative changes in the volume of a-SiO_2 samples under pressure are shown in figure 9. The room temperature curves [68] are also presented for comparison. Starting at a certain moment of the pressure increase, the curves deviate from their standard regular behaviour corresponding to linear changes in the bulk modulus. This is most clearly seen from the softening of the bulk modulus (figures 9(b) and (d)). The higher the temperature, the earlier the compressibility anomaly is observed, starting at pressures of 5.7 and 6.7 GPa and at temperatures of 475 and 545 K, respectively. As the pressure is reduced, the behaviour of the a-SiO_2 volume becomes essentially irreversible, because the glass compressibility of the new state diminishes. As a result, a large residual densification ($\sim$5 and 12% in the experiments presented in figures 9(a) and (c), respectively) is observed in normal conditions.

Summing up the results of the *in situ* measurements of the a-SiO_2 volume [36], we succeeded in determining rather accurately the region corresponding to the structural transition to a denser a-SiO_2 modification of the phase diagram. The extrapolation of the data obtained in this work to the high-temperature region suggests that, at high temperatures near the crystallization temperature, the structural densification of a-SiO_2 occurs near 3–4 GPa. The temperature interval of the reverse transformation to a less dense glass was estimated using isochronous annealing of the prepared densified glasses at normal pressure and was found to be equal to 1000–1100 K (for an annealing rate of 20 K min^{-1}).

The transformation resulting in the residual glass densification of a-SiO_2 is accompanied, directly under pressure, by a small (a few per cent) change in the volume and is fully irreversible. Formally, much of the residual glass densification at normal conditions is due to a significantly lower compressibility of a-SiO_2 after transformation (figure 9). At atmospheric pressure, the bulk modulus of the glass with the maximum (18%) residual densification is higher by 80% than in the initial glass. It has become clear that the processes of irreversible densification in a-SiO_2 at pressures exceeding 9 GPa at room temperature, and at high temperatures and lower pressures of 5–7 GPa, are caused by the same structural transformation.

We conclude that at least two pressure- and temperature-diffuse transformations accompanied by significant changes in the structure and properties of a-SiO_2 should exist at pressures below 40 GPa (figure 10). By analogy with the quartz–coesite phase transition, the first transformation does not noticeably distort the SiO_4 tetrahedra and short-range-order structure for Si atoms, but it is accompanied by changes in the topology of packing of the SiO_4 tetrahedra. It is irreversible at room temperature and brings about the residual densification. The second transformation occurs at higher pressures. It is accompanied by a change in the silicon coordination from tetrahedral to octahedral, by analogy with the coesite–stishovite phase transition, and is reversible at room temperature. The diagram for both transformations in a-SiO_2, constructed using the currently discussed experimental results and the literature data (see references in [36]), is presented in figure 10. At room temperature, the pressures of the two transformations overlap, whereas the reverse transitions are well separated (figure 10). The presence of two different modifications in a-SiO_2 allows one to explain all currently available experimental data concerning the behaviour of compressed glassy silica [11–14, 25, 78–81] and, at the same time, agrees well with the existing model calculations [82–88].

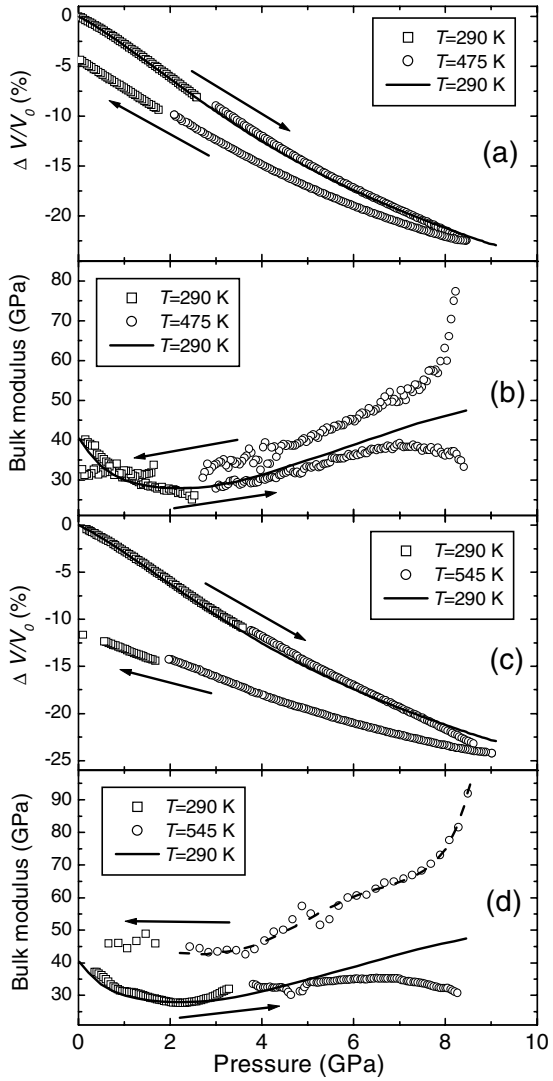

Figure 9. The study of a-SiO_2 at high pressures and high temperatures [36]. ((a), (c)) Relative changes of the a-SiO_2 volume in the compression and decompression cycles (the initial and final portions were measured at room temperature) and ((b), (d)) the corresponding bulk moduli obtained by the numerical differentiation of volume curves (for $T = 475$ K, the curves were differentiated directly, and for $T = 545$ K, the curves were smoothed out before the differentiation because of the enhanced noise level). The data corresponding to the a-SiO_2 compression at room temperature are given for comparison.

4.2. Amorphous H_2O ices

The hda-to-lda and lda-to-hda transformations in amorphous ice were studied mainly by the ultrasonic method [89–91] using a high-pressure ultrasonic piezometer [37]. The hda-to-lda transformation upon heating is of an unusual character. One can select three distinct stages of the hda-to-lda transformation (figure 11), namely the shear elastic softening (from ≈100 K), the bulk softening (from ≈115 K), and the main volume jump (starting at ≈127 K). The data on

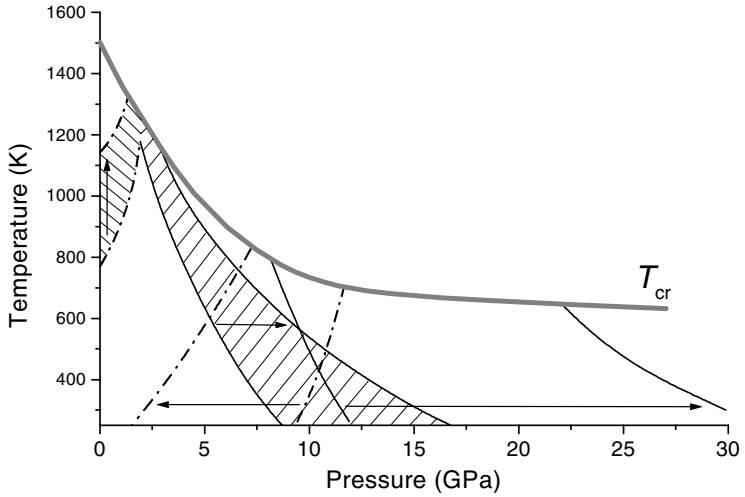

Figure 10. The pressure–temperature phase diagram for the transformations of glassy a-SiO_2 below the crystallization temperature T_{cr} (see details in [36]). These data are evidence for the two transitions: between the ordinary and densified tetrahedral phases (the hatched regions correspond to the direct and reverse transitions) and between the densified tetrahedral and octahedral phases (non-hatched regions). The regions of direct transitions are bounded by the solid lines, and the regions of reverse transitions are bounded by the dot-and-dash curve. The boundaries of transition regions are drawn rather arbitrarily. The arrows show the directions of the corresponding transitions.

the shear modulus G indicate that the shear instability plays an important role in the AAT mechanism. However, one should take into account that the shear and bulk softening may be not only a precursor of the hda-to-lda transformation, but also a natural consequence of the structural transformation to a less dense and softer lda phase. The time-dependent study of hda ice at fixed temperatures [91] indicates that some irreversible relaxation occurs in the interval 100–130 K that is accompanied by a decrease of the density and shear modulus. But reverse thermo-cycles (when the temperature was decreased and then increased again) showed that the transverse velocity V_t and modulus G softening with temperature (in the interval 100–130 K) were partially reversible in the interval 100–120 K (figure 12) [91]. Thus, the elastic softening of hda ice is not only a result of irreversible relaxation, but it is also an inherent property of the hda amorphous network and should be considered an elastic precursor for the hda-to-lda transformation.

The transverse ultrasonic velocity and density were measured during the compression of lda ice and then upon its decompression. The lda-to-hda transition begins at $\approx$0.4 GPa($T =$ 110 K) in accordance with the previous studies [18, 20]. However, the transformation does not finish at these pressures and continues at least up to 1.4 GPa. This is proved, first, by the comparison of the direct and reverse dependences and, second, by the relaxation measurements. We maintained the pressure for $\sim$1–2 min at higher values and found the following relaxation changes: $\sim$0.2–1.0% for density and $\sim$0.3–2.0% for V_t. The most striking observation consists in the shear elastic softening of the lda phase up to the lda-to-hda transition onset. The pressure derivative for the shear modulus for lda phase, $G'_P \approx -(0.3–0.6)$, is very close to that for 1h ice, $G'_P \approx -(0.4–0.6)$. There is a clear similarity between the 1h-to-hda and lda-to-hda transformations.

A common feature of the lda-to-hda and hda-to-lda transformations is the elastic softening as a structural change precursor. However, there is a clear difference in scenario between

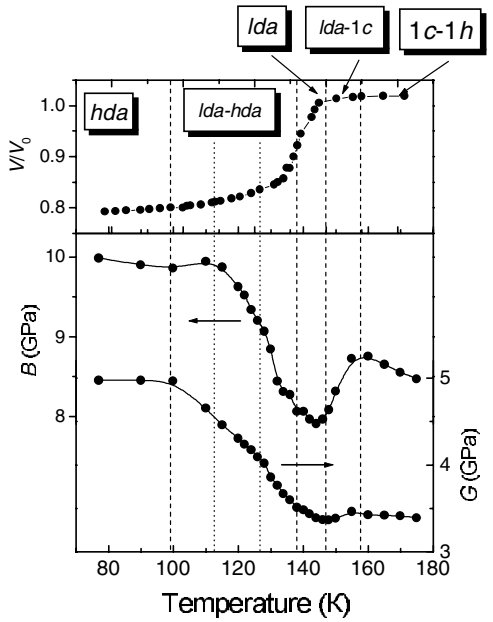

Figure 11. The relative volume $\Delta V/V$, bulk modulus B, and shear modulus G at 0.05 GPa during temperature-induced hda-to-lda transformation [89].

these transformations. The hda-to-lda transition is of a gradual stepwise character (figure 12), because before the volume jump, the transformation starts from the elastic softening as both an inherent property of the amorphous network and as a result of the irreversible relaxation. The lda-to-hda transition is quite different, and one can choose two distinct stages: the first of them corresponds to pressurizing of the lda phase with the predominantly reversible elastic softening as an inherent property of the lda network, and the second one is the structural transformation starting rather abruptly.

It is natural to consider the lda–hda transition as a low-temperature continuation of the first-order transition in supercooled water (figure 13) [8]. However, the wide tail of the pressure-induced lda-to-hda transformation, as well as a complicated picture of the temperature-induced hda-to-lda transformation with the relaxation precursor (figure 13) cannot be interpreted in the framework of an ordinary first-order transition.

4.3. Summary remark

So, the kinetics of AAT in SiO_2 and GeO_2 glasses display a number of anomalous phenomena, in particular the logarithmic kinetics of densification at a fixed pressure. Ultrasonic study of H_2O ice also shows a number of unusual features in the kinetics of lda–hda transformations, such as the three-stage (shear and bulk softening and volume jump) scenario of the temperature-induced hda-to-lda transformation, precursor relaxations, and the relaxation tail after the transformation. The recent inelastic neutron scattering study of amorphous polymorphism in ice [92] confirms a complicated non-ergodic nature of the lda–hda transformation and its 'non-first-order' kind of transition.

Thus, transformations with specific features, distinguishing them both from first-order phase transitions in crystals and from sharp transformations in melts, are possible in amorphous

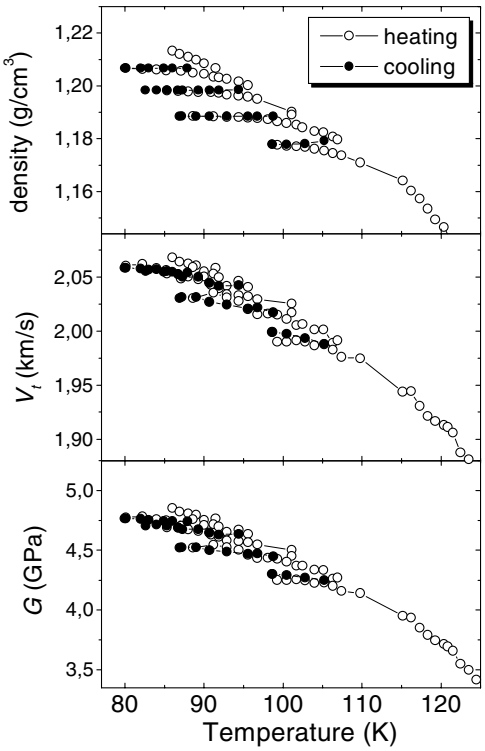

Figure 12. Temperature dependences of the density, transverse sound velocity V_t, and shear modulus for thermo-cycles during hda-to-lda transformations [91].

solids under compression. It should be emphasized that transformations in amorphous solids take place far away from the conditional thermodynamic equilibrium and can have the characters of both jump-wise changes of properties and diffuse anomalies. These different transition scenarios will be discussed below.

5. Discussion

The possibility of relatively sharp or quite sharp transformations in a number of melts of elementary substances and simple compounds is now beyond doubt from the experimental standpoint. However, from the theoretical view, the problem of the order parameter for such transformations remains unresolved and we still need criteria and rules selecting the type of melt in which such transformations can take place.

A strong anisotropy or the energy hierarchy in the structure-forming part of the interaction potential seems to be one of the necessary conditions for realizing the first-order phase transition in a liquid. Typical examples are the strong orientation anisotropy, the strong three-particle interaction leading to substantial angular correlations, and the presence of a hierarchy in the interactions between different types of atoms in molecular liquids. The existence of a weaker structure-forming interaction determines the system melting, while a stronger interaction ensures the existence of the order parameter (i.e., correlation) characterizing the whole system.

A useful microscopic theory of phase transitions in isotropic liquids is not developed yet, and only empirical models and computer simulations have been used in practice to date [3]. The model of a regular solution, based on the assumption that different kinds of atom could exist in

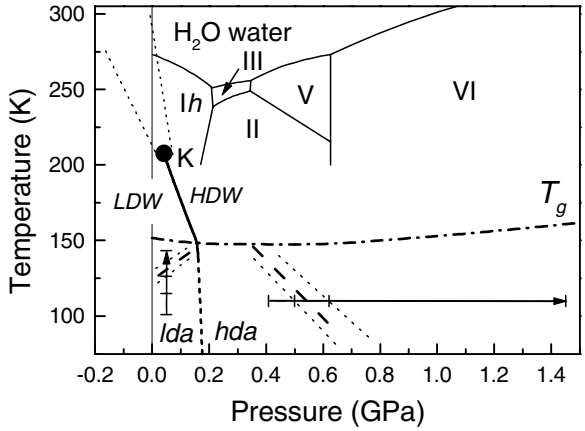

Figure 13. The hypothetical phase diagram of supercooled water in the equilibrium phase diagram of ice. The line of the first-order phase transition (the thick solid line) between low-density (LDW) and high-density water (HDW) terminates at the critical point K [8]. At a higher temperature, it transforms to the region of anomalous properties of liquid water (dotted lines); at lower temperatures (below the glass transition or crystallization temperature T_g) to the line (short dashed line) of thermodynamic equilibrium between glassy lda and hda ices. The real lda-to-hda transformations are shown by the arrows, indicating the transition width and including the relaxation precursor, interval of softening, and relaxation tail. The position of the main volume jump for AATs and its width are shown by the long chain and dotted lines, respectively.

the same liquid substance, was the first attempt to describe the transitions in liquids [93, 94]. This model could show the possibility of a first-order transition in liquids with the critical point at high temperatures. However, there is no microscopic basis for such an empirical model, because the existence of the different forms of the same atom is a physically groundless assumption.

Because the transitions in liquids occur in fact between phases with the definite short-range order, the most natural theoretical approximation should involve the concept of liquids with long-living medium-range-order fluctuations (cluster) with a certain short-range-order structure. During the last 50 years, many authors have proposed empirical models of liquids, considering them as systems which are heterogeneous at the nanometre scale and composed of long-living crystal-like clusters embedded in a gas-like isotropic part [95]. Liquid–glass transition could be considered in these terms as percolation through the corresponding clusters during temperature decrease [96]. The size of the similarly introduced clusters defines the pressure and/or temperature widths of possible liquid–liquid transitions [97]. Introducing the interaction between clusters as a specific contribution to the free energy, it is possible to describe the first-order transition in liquids terminated by the critical point at high temperatures. A more consistent and detailed empirical model of cooperative medium-range bond ordering (clustering) for any liquid was developed by Tanaka in [98] (see also references therein), where two kinds of order parameter, density and local bond order, were supposed for liquid state. Unfortunately, this model is still phenomenological and does not provide an understanding of the microscopic mechanism for the competition between the two types of bond ordering realized in a liquid–liquid transition.

There have been very few attempts to describe the transitions in liquid from the microscopic point of view, taking into account the interatomic potentials and certain short-range-order structures. In particular, it was shown in [99] that the bond orientation long-range order could

exist in the supercooled state of liquid with a Lennard-Jones interparticle potential. The study of systems with double-step or shoulder-type interparticle potentials also clarifies a possible microscopic origin of the first-order liquid–liquid phase transition (see [100] and references therein). The spinodals for the phase transitions in liquid with a shoulder-type interatomic potential are obviously related to the volume instability condition (bulk modulus equal to zero, $B = 0$). The specific instabilities, related to specific kinds of atomic ordering, could exist in liquid with some kind of hidden symmetry in addition to the thermodynamic stability loss ($B = 0$). The theoretical description in this case should be reduced to the analysis of the three- and four-particle distribution functions [99].

As for the transformations in amorphous solids, the situation here remains obscure, both from the experimental and from the theoretical point of view. For describing the transitions in amorphous solids it is necessary to elaborate a new terminology taking into account the specific character of the metastable amorphous state. The concept of the first-order amorphous–amorphous transition is based primarily on the postulating of two distinctly separate low-density and high-density potential energy megabasins (figure 14) over the entire pressure range, where pressure changes their mutual energy levels. However, another scenario is possible, if the minimum megabasin continuously transforms from the low-density to the high-density state with pressure increase (figures 14 and 15). This means that the amorphous states with intermediate coordination (in particular, the atomic-level mixture of two amorphous structure types) and density are preferable thermodynamically in the transition pressure range, whereas the pure low-density and high-density phases can exist only far from the transition region. With pressure change, the Gibbs free energy gradually diminishes (figure 15), the local coordination changes occurring in the most stressed part of the network [101]. The possibility of the scenario discussed is in agreement with theoretical and experimental studies [68, 85, 87, 101, 102].

The proposed diffuse scenario of a transformation in the amorphous solid is defined not by the thermodynamic equilibrium, but by the softening of particular phonon modes (local spinodals [17, 68, 85, 101]) responsible for a local rearrangement of the amorphous network. A finite width of the AAT naturally results from a wide dispersion of geometrical and topological characteristics of the amorphous networks [103] and, consequently, from a dispersion of the atomic-level energy and dynamic characteristics [104–106]. In contrast to the case for liquids, the width of the AAT depends to a degree on the distribution of local static atomic-level stresses in the amorphous network [101, 104–106]. Thus, the AAT kinetics should be quite different from the corresponding liquid–liquid transition above the glass-forming temperature. A wide variation of geometric characteristics results in a wide distribution of atomic energies and stresses (for example, see [104–106]). The external pressure increase should upset the distribution of energy barriers, preventing the reconstruction of short-range order, and soften the open-packed networks such as those in SiO_2 and GeO_2 glasses. A wide distribution of local pressure spinodals [17, 68, 85, 101] with respect to the coordination change corresponds to the softening of different network parts at different pressures. The atomic-level stress tensor [107] seems to be a governing parameter for the instability of local network parts. Thus, the local instability approach allows one to explain the observed anomalous features of AATs on the basis of distributions of energy (transformation barriers) and dynamic (the tensor of atomic-level stresses) characteristics and considering glasses as non-ergodic systems.

As we already noted, in a number of amorphous substances, such as a-SiO_2, a-GeO_2, and amorphous carbon phases, transformations occur across a very wide range of pressures [11–17, 21, 22], whereas fairly sharp transformations, formally similar to jump-wise first-order phase transitions, take place in some other amorphous substances, such as a-H_2O and a-D_2O [18–20, 108, 109]. A wide range of transformations in amorphous solids would of necessity stem from the nanometre-scale dispersion of structural characteristics in amorphous

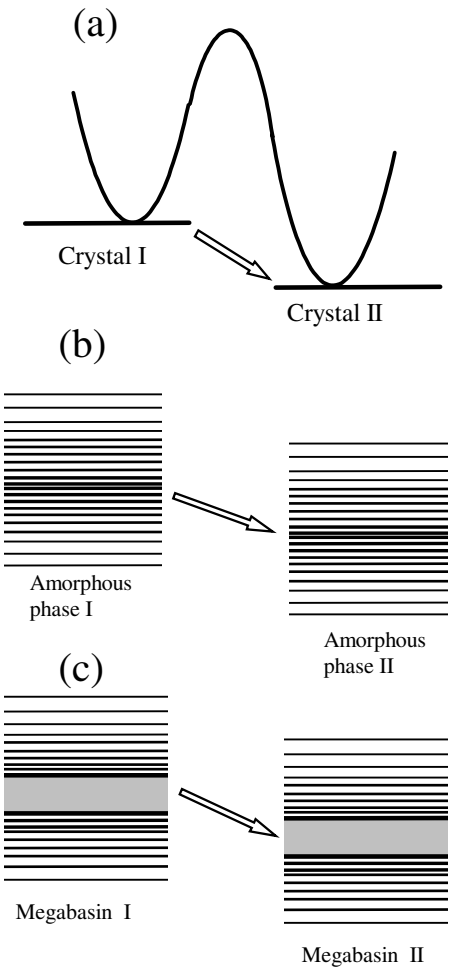

Figure 14. The energy diagram for the interaction between (a) crystalline phases and ((b), (c)) amorphous phases. The diagrams for the amorphous phases show energy levels for individual elementary clusters or atoms (b) as the discrete dispersed levels or (c) as the energy bands for amorphous megabasins, where the individual levels show defect atomic states with respect to the ideal amorphous phase.

materials [68, 91, 104–106]. At the same time, the reason for the existence of the sharp transformation scenario for transitions between amorphous phases, as, for instance, in a-H_2O, is at first sight incomprehensible. In [110] it has been shown for disordered systems of simple particles that the specific features of the central potential can directly determine whether there is a sharp or diffuse type of transformation between low-density and high-density amorphous phases. In order to understand the specificity of the transition scenario in a real substance, it is necessary to consider the nanometre-scale mechanism of the new phase formation.

Since diffusion processes in amorphous materials are strongly frozen, the new phase formation can proceed only through the formation of nuclei without their noticeable growth. At the same time, the formation of nuclei of a new amorphous modification inside the parent amorphous phase has a distinctive feature associated with the presence of ‘frozen’ quasi-static

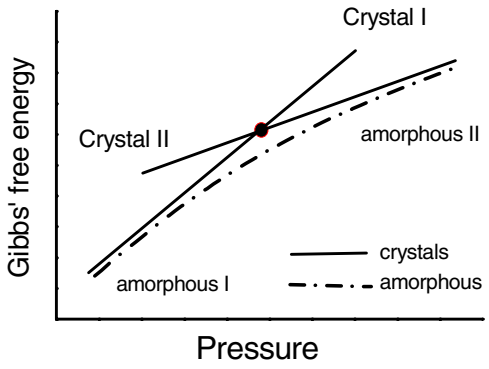

Figure 15. The intersection of the Gibbs free energy curves for two crystalline phases and the smooth gradual transformation between the curves for two amorphous phases. Conditionally, the asymptotic dependences for Gibbs free energies of amorphous phases are chosen to be the same as curves for crystalline phases.

stresses at the atomic level in the amorphous network. The presence of these stresses may lead to the distribution of the corresponding energies W expended in the formation of nuclei of the new phase in various parts of the amorphous network [111]. The distribution of the W-values in amorphous substances will result in different $W(P)$ dependences, and, consequently, at different parts of the amorphous network the intense formation of a new phase starts at different pressures. At the same time, the dispersion of structural characteristics and properties in the amorphous phase leads to a wide distribution of the W-values only in the case where the critical nucleus size $r_{\min}$ is less than the size of the domain of structural correlations in an amorphous substance [111], i.e., $r_{\min} < a_c$, where a_c is the radius of structural correlations (correlation length). However, in the case where the critical nucleus size exceeds the correlation length in the amorphous phase, the substance may be regarded as a uniform continuous medium with quite narrow dispersion of W-values [111], since the atomic-level stresses are averaged over nucleating domains. The kinetics of transformations between amorphous modifications will be in this case the same as for ordinary first-order phase transitions, i.e. the transformation will occur sharply with pronounced separation of domains of the parent and product amorphous phases. Therefore, different relationships between the values of $r_{\min}$ and a_c will result in qualitatively different kinetic scenarios of the transition.

The correlation length in the amorphous state does not depend too strongly on the specific substance and usually amounts to 6–10 coordination spheres, i.e., 15–25 Å [103]. At the same time, the critical grain sizes of new amorphous modifications can differ substantially for various substances and are primarily defined by the lattice geometry and interatomic forces. We performed the respective evaluations for transformations in the amorphous state for a-H_2O, a-SiO_2, and a-GeO_2 on the basis of data obtained for the transition parameters and for the elastic moduli of the corresponding phases.

The critical nucleus size ($r_{\min} \sim$ 20–40 Å) for amorphous ice is comparable to the correlation length in the initial amorphous phase or slightly exceeds it. As a consequence, the W-value is nearly the same for different parts of the amorphous phase, and the lda–hda transformation proceeds rapidly, similarly to a first-order transition (the transition width $\Delta P^* \leqslant 0.05$ GPa) and with clear separation of the two phases [19, 108]. For the transformation between the amorphous phases of SiO_2 with the fourfold and sixfold coordination of silicon atoms, $r_{\min} \sim$ 5–10 Å, which is noticeably less than the radius of structural correlations. As

a consequence, the W-value has a sufficiently wide distribution over different parts of the amorphous network, and the transformation in a-SiO_2 occurs in a wide range of pressures $\Delta P^* \sim 10$ GPa. The transformation in GeO_2 glass occupies an intermediate position, but also with a wide dispersion of W-values.

Thus, the mechanism of formation of nuclei of the new amorphous phase directly determines the scenario of the high-pressure transformation. The density of low-frequency modes (particularly, floppy modes) may be directly related [89, 112] to the high-pressure dynamics of the amorphous phase, and specific features of the low-frequency and floppy mode spectra of glassy SiO_2 [113], lda and hda H_2O ices [114], etc, define the different scenarios of transformations in a-SiO_2, on one hand, and in amorphous ices, on the other hand. In particular, the geometrical differences in interaction in the amorphous networks of a-SiO_2, a-GeO_2, and amorphous ices can be considered in terms of the mechanical network rigidity and rigidity percolation from soft to rigid amorphous networks.

A similar consideration of two transformation regimes, sharp and diffuse, can be applied to the liquid state as well as in the framework of cluster-based models. The ratio between the size of the structural correlations and the minimal size of new phase clusters, corresponding to a decrease of the Gibbs free energy in liquid, would be a critical parameter in this case.

Using this idea, it is possible to predict the character of hypothetical phase transformations in various amorphous and liquid substances. For instance, the transformations in chalcogenide glasses, such as Se and S ($Z \approx 2$) at low temperatures, should be very broad in pressure. In turn, the possible AAT (at temperatures below those of the crystallization of amorphous phases) in topologically rigid tetrahedral amorphous semiconductors ($Z \sim 4$), such as a-Si and a-Ge, should be evidently sharp (see in this respect [115]).

In contrast to the case for amorphous phases, large atomic stresses in the disordered liquid state exist only for very short time intervals. However, for ordinary experimental times, these stresses have negligible averages for the shear components. For this reason, the liquids including their supercooled states are elastically relaxed systems without the macroscopic static shear elasticity. In the glassy states, atomic stresses are frozen, and amorphous phases have elasticity similar to that in crystals. Therefore, despite common features of transformations in the liquid and amorphous states, such as a change of the short-range-order structure (possibly diffuse or sharp) and anomalies or changes in thermodynamic and kinetic properties, amorphous and glass solids do not represent simple analogues of supercooled melts, particularly in the detailed kinetics of their transformations.

As already noted, there are virtually no examples of comprehensive experimental studies comparing transitions between liquid phases, including the region of supercooled states, and transformation in the relevant amorphous solids for the same substance, due to natural experimental difficulties. It is assumed that the direct and reverse transformations in a-H_2O occurring far from equilibrium under pressure (at $P \approx 5$ and $\approx$1 kbar at $T \leqslant 140$ K, respectively) are genetically related to the sharp transitions in supercooled water at higher temperatures and pressures $P \approx$ 1–2 kbar [8, 18–20, 89–91]. However, the transformation in supercooled water itself has been studied only by indirect methods [116] or computer simulations (see references in [8]).

It may only be suggested that the diffuse direct and reverse transformations in a-GeO_2 from the quartz-like to the rutile-like phase are associated with the corresponding hypothetical transformations in the melt at $P \approx$ 2–4 GPa (figure 4). The existence of a sharp transition in the supercooled liquid state of GeO_2, as well as the possibility of existence of the corresponding critical point, remains open to question. Note that the coordination change in the disordered phases of GeO_2 takes place at higher pressures than in the crystal, which is associated with the high energy of disordering of the rutile-like modification [117].

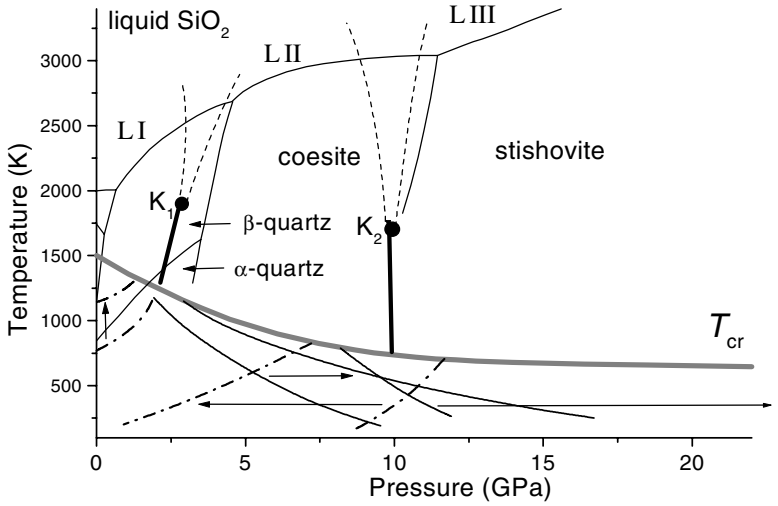

Figure 16. The thermodynamic phase diagram of SiO_2 and the hypothetical diagram of liquid SiO_2 with two possible first-order phase transitions in a supercooled liquid state and two corresponding critical points (K_1 and K_2). The liquid–liquid phase transitions correspond to the broadened regions of structural rearrangement (between the states LI, LII, and LIII) in the ordinary liquid and, below the temperature T_{cr}, to the transitions between the amorphous states labelled according to figure 10.

The conclusion of two transformations in a-SiO_2 (figure 9) allows one to make another assumption about the phase diagram of SiO_2 (figure 16). It is natural to assume that two analogous transformations occur in the SiO_2 melt. This is indirectly confirmed by the data reported in [51, 53–55], where the first transition was shown as a change in the degree of densification for glasses prepared by quenching from a melt under pressure [53], and the second transition was associated with a substantial rearrangement of the atomic short-range order and caused anomalous properties of the SiO_2 melt [51, 54, 55]. In turn, the assumption can be made that two first-order phase transitions and the corresponding critical points may exist in the supercooled SiO_2 liquid (figure 16). Vice versa, it is possible that the transformations in liquid SiO_2 would be diffuse until the zero temperature was reached, like the transitions in the amorphous state. A possibility of sharp transitions in supercooled liquid SiO_2 and clarification of the positions of the corresponding critical points call for additional experimental and theoretical studies.

The presence of two transitions in the amorphous and liquid state represents a phenomenon which is, presumably, typical for other substances where a hierarchy of pressure-induced phase transitions in the crystal state are accompanied by a change in the topology of sub-molecular ordering followed by a change in the short-range order and in the type of atomic packing. For instance, the occurrence of the second transition between the amorphous phases may be expected for H_2O at higher pressures and low temperatures.

6. Conclusions

Summarizing, one can state that the study of phase transitions in disordered condensed media is in many respects at the initial stage at the moment, and this status is already reflected even in the terminology problems [118]. The development of the concept of the order parameter for liquids and the correct description of static stresses in amorphous solids will play a key role in the future progress of the theory in this area.

Despite numerous experimental examples of sharp variations in the properties and structure of melts, a clear identification of liquid–liquid transformations as first-order transitions is still lacking, and additional powerful experimental and theoretical arguments are required, e.g., for liquid selenium, sulfur, and carbon. Theoretical models and criteria unambiguously predicting possible first-order or smoothed liquid–liquid transformations in relatively simple liquids still have to be developed.

Further developments in the glass-forming theory will probably become the bridge that will relate the liquid–liquid and AATs. In the process of vitrification, static stresses appear to be the bridge that will relate the liquid–liquid and AATs. In the process of vitrification, static stresses appear in liquids that completely alter the pattern of transformations and determine their specific features. As a consequence, transformations in amorphous solids proceed far away from the conditional thermodynamic equilibrium, and the kinetic scenario (sharp or smooth transformations) is governed by the character of the interparticle interaction in particular amorphous systems. Unusual features of transformations in amorphous solids, such as the logarithmic kinetics, negative hysteresis, and long transformation tails, are also connected with the presence of frozen static stresses, as well as the metastability and non-ergodicity of amorphous substances.

Acknowledgments

The authors are grateful to S M Stishov, S V Popova, R N Voloshin, V N Ryzhov, O B Tsiok, E L Gromnitskaya, O V Stal'gorova, and F S El'kin for helpful discussions. The work was supported by the Russian Foundation for Basic Research (project Nos 01-02-16557 and 02-02-16298) and INTAS (project 00-807).

References

[1] Brazhkin V V, Popova S V and Voloshin R N 1997 *High Pressure Res.* **15** 267
[2] De Gennes P 1974 *The Physics of Liquid Crystals* (London: Oxford University Press)
[3] Brazhkin V V, Buldyrev S V, Ryzhov V N and Stanley H E (ed) 2002 New kinds of phase transitions: transformations in disordered substances *Proc. NATO Advanced Research Workshop (Volga River, Moscow, May 2001)* (Dordrecht: Kluwer)
[4] Katayama Y, Mizutani T, Utsumi W, Shimomura O, Yamakata M and Funakoshi K 2000 *Nature* **403** 170
[5] Brazhkin V V, Popova S V and Voloshin R N 1989 *JETP Lett.* **50** 362
[6] Brazhkin V V, Voloshin R N, Popova S V and Umnov A G 1991 *Phys. Lett.* A **154** 413
[7] Mezouar M, Crichton W, Monako G, Falconi S, Occelli F, Bouvier P and Crapanzano L 2002 *40th European High Pressure Research Group Mtg (Edinburgh, UK, Sept. 2002) (Abstracts)* (Edinburgh: The University of Edinburgh) p 34
[8] Mishima O and Stanley H E 1998 *Nature* **396** 329
[9] Glosli J N and Ree F H 1999 *Phys. Rev. Lett.* **82** 4659
[10] Togaya M 1997 *Phys. Rev. Lett.* **79** 2474
[11] Grimsditch M 1984 *Phys. Rev. Lett.* **52** 2379
[12] Hemley R J, Mao H K, Bell P M and Mysen B O 1986 *Phys. Rev. Lett.* **57** 747
[13] Meade C, Hemley R J and Mao H K 1992 *Phys. Rev. Lett.* **69** 1387
[14] Zha C S, Hemley R J, Mao H K, Duffy T S and Meade C 1994 *Phys. Rev.* B **50** 13105
[15] Itie J P, Polian A, Calas G, Petiau J, Fontaine A and Tolentino H 1989 *Phys. Rev. Lett.* **63** 398
[16] Durben D J and Wolf G H 1991 *Phys. Rev.* B **43** 2355
[17] Smith K H, Shero E, Chizmeshya A and Wolf G H 1995 *J. Chem. Phys.* **102** 6851
[18] Mishima O, Calvert L D and Whalley E 1985 *Nature* **314** 76
[19] Mishima O, Takemura K and Aoki K 1991 *Science* **254** 406
[20] Mishima O 1994 *J. Chem. Phys.* **100** 5910
[21] Aleksandrov I V, Goncharov A F, Yakovenko E V and Stishov S M 1992 *High-Pressure Research: Application to Earth and Planetary Sciences* ed Y Syono and H Manghnani (Washington, DC: American Geophysical Union) p 409

[22] Lyapin A G, Brazhkin V V, Lyapin S G, Popova S V, Varfolomeeva T D, Voloshin R N, Pronin A A, Sluchanko N E, Gavrilyuk A G and Trojan I A 1999 *Phys. Status Solidi* b **211** 401
[23] Uhlmann D R, Hays J F and Turnbull D 1967 *Phys. Chem. Glasses* **8** 1
[24] Park J B and Uhlmann D R 1970 *J. Non-Cryst. Solids* **7** 438
[25] Grimsditch M 1986 *Phys. Rev.* B **34** 4372
[26] Williams Q and Jeanloz R 1988 *Science* **239** 902
[27] Polian A and Grimsditch M 1990 *Phys. Rev.* B **41** 6086
[28] Grimsditch M, Bhadra R and Meng Y 1988 *Phys. Rev.* B **38** 7836
[29] Wolf G H, Wang S, Herbst C A, Durben D J, Oliver W F, Kang Z C and Halvorson K 1992 *High-Pressure Research: Application to Earth and Planetary Sciences* ed Y Syono and H Manghnani (Washington, DC: American Geophysical Union) p 503
[30] Khvostantsev L G, Vereshchagin L F and Novikov A P 1977 *High Temp.–High Pressure* **9** 637
[31] Brazhkin V V, Umnov A G, Voloshin R N and Popova S V 1994 *High Pressure Res.* **13** 61
[32] Brazhkin V V, Umnov A G, Voloshin R N and Popova S V 1994 *High Pressure Res.* **13** 297
[33] Brazhkin V V and Popova S V 1989 *Rasplavy* **4** 97
[34] Brazhkin V V, Larchev V I, Popova S V and Skrotskaya G G 1989 *Phys. Scr.* **39** 338
[35] Tsiok O B, Bredikhin V V, Sidorov V A and Khvostantsev L G 1992 *High Pressure Res.* **10** 523
[36] El'kin F S, Brazhkin V V, Khvostantsev L G, Tsiok O B and Lyapin A G 2002 *Pis. Zh. Ekp. Teor. Fiz.* **75** 413 (Engl. transl. 2002 *JETP Lett.* **75** 342)
[37] Stal'gorova O V, Gromnitskaya E L, Dmitriev D R and Voronov F F 1996 *Prib. Tekh. Eksp.* **39** 115 (Engl. transl. 1996 *Instrum. Exp. Tech.* **39** 880)
[38] Voronov F F, Stal'gorova O V and Gromnitskaya E L 1994 *Zh. Eksp. Teor. Fiz.* **105** 1456 (Engl. transl. 1994 *JETP* **78** 785)
[39] Brazhkin V V, Voloshin R N, Popova S V and Lyapin A G 2002 *New Kinds of Phase Transitions: Transformations in Disordered Substances* ed V V Brazhkin, S V Buldyrev, V N Ryzhov and H E Stanley (Dordrecht: Kluwer) p 239
[40] Brazhkin V V, Voloshin R N, Popova S V and Umnov A G 1991 *High Pressure Res.* **6** 363
[41] Brazhkin V V, Voloshin R N, Popova S V and Umnov A G 1992 *J. Phys.: Condens. Matter* **4** 1419
[42] Brazhkin V V, Voloshin R N and Popova S V 1992 *Phys. Lett.* A **66** 383
[43] Brazhkin V V, Voloshin R N, Popova S V and Kalyaeva N V 1991 *High Pressure Res.* **6** 341
[44] Brazhkin V V, Voloshin R N, Popova S V and Umnov A G 1992 *High Pressure Res.* **10** 454
[45] Brazhkin V V, Popova S V and Voloshin R N 1999 *Physica* B **265** 64
[46] Brazhkin V V, Umnov A G, Voloshin R N and Popova S V 1994 *High Pressure Res.* **13** 61
[47] Brazhkin V V, Dmitriev D R and Voloshin R N 1994 *Phys. Lett.* A **193** 102
[48] Vezzoli G C, Dachille F and Ray R 1965 *Polym. Sci.* A **17** 1557
[49] Clarke J H, Dore J C, Granada J R, Reed J and Walford G 1981 *Mol. Phys.* **42** 861
[50] Senda Y, Shimojo F and Hoshino K 2002 *J. Phys.: Condens. Matter* **14** 3715
[51] Saika-Voivod I, Sciortino F and Poole P H 2000 *Phys. Rev.* E **63** 11202
[52] Shell M S, Debenedetti P G and Panagiotopoulos A Z 2002 *Phys. Rev.* E **66** 11202
[53] Kanzaki M 1990 *J. Am. Ceram. Soc.* **73** 3706
[54] Zhang J, Liebermann R C, Gasparik T, Herzberg C T and Fei Y 1993 *J. Geophys. Res.* **98** 19785
[55] Ohtani E, Taulelle F and Angell C A 1985 *Nature* **314** 78
[56] Hemley R J, Badro J and Teter D M 2000 Polymorphism in crystalline and amorphous silica at high pressures *Physics Meets Mineralogy* ed H Aoki *et al* (Cambridge: Cambridge University Press) p 173
[57] Tonkov E Yu 1992 *High Pressure Phase Transformations. A Handbook* vols 1, 2 (Philadelphia, PA: Gordon and Breach) (1988 (Moscow: Metallurgiya))
[58] Brazhkin V V, Voloshin R N, Lyapin A G and Popova S V 2003 *Phys.–Usp.* at press
[59] Jackson I 1976 *Phys. Earth Planet. Inter.* **13** 218
[60] Sharma S K, Virgo D and Kushiro I 1979 *J. Non-Cryst. Solids* **33** 235
[61] Feltz A 1983 *Amorphe und Glasartige Anorganische Festkörper* (Berlin: Akademie) (Engl. transl. 1993 *Amorphous Inorganic Materials and Glasses* (Weinheim: VCH))
[62] Mackenzie J D and Claussen W F 1961 *J. Am. Ceram. Soc.* **44** 79
[63] Uhlmann D R 1972 *J. Non-Cryst. Solids* **7** 337
[64] Brazhkin V V 1987 Influence of high pressure on the solidification of metallic melts *PhD Thesis* Moscow Physical and Technical Institute
[65] Endo H, Tamura K and Yao M 1987 *Can. J. Phys.* **65** 266
[66] Roberts C J, Panagiotopoulos A Z and Debenedetti P G 1996 *Phys. Rev. Lett.* **77** 4386
[67] Poirier J P 1985 *Nature* **314** 12

[68] Tsiok O B, Brazhkin V V, Lyapin A G and Khvostantsev L G 1998 *Phys. Rev. Lett.* **80** 999
[69] Stal'gorova O V, Gromnitskaya E L, Brazhkin V V and Lyapin A G 1999 *Pis. Zh. Eksp. Teor. Fiz.* **69** 653 (Engl. transl. 1999 *JETP Lett.* **69** 694)
[70] Lyapin A G, Brazhkin V V, Gromnitskaya E L, Stal'gorova O V and Tsiok O B 1999 *Usp. Fiz. Nauk* **169** 1157 (Engl. transl. 1999 *Phys.–Usp.* **42** 1059)
[71] Schroeder J, Bilodeau T G and Zhao X S 1990 *High Pressure Res.* **4** 531
[72] Suito K, Miyoshi M, Sasakura T and Fujisawa H 1992 *High-Pressure Research: Application to Earth and Planetary Sciences* ed Y Syono and H Manghnani (Washington, DC: American Geophysical Union) p 219
[73] Murani A P 1985 *J. Phys. F: Met. Phys.* **15** 417
[74] Theye M L, Gheorghiu A, Gandais M and Fisson S 1980 *J. Non-Cryst. Solids* **37** 301
[75] Tsiok O B, Sidorov V A, Bredikhin V V, Khvostantsev L G, Troitskiy V N and Trusov L I 1995 *Phys. Rev.* B **51** 12127
[76] Karpov V G and Grimsditch M 1993 *Phys. Rev.* B **48** 6941
[77] Ginzburg S L 1989 *Irreversible Phenomena of Spin Glasses* (Moscow: Nauka)
[78] Hemley R J, Prewitt C T and Kingma K J 1994 *Silica: Physical Behavior, Geochemistry and Materials Applications* (*Reviews in Mineralogy*) vol 29, ed R J Hemley, C T Prewitt and G V Gibbs (Washington, DC: Mineralogical Society of America) p 41
[79] Bridgman P W and Simon I 1953 *J. Appl. Phys.* **24** 405
[80] Cohen H M and Roy R 1965 *Phys. Chem. Glasses* **6** 149
[81] Gerber Th, Himmel B, Lorenz H and Stachel D 1988 *Cryst. Res. Technol.* **23** 1293
[82] Stixrude L and Bukowinski M S T 1991 *Phys. Rev.* B **44** 2523
[83] Tse J S, Klug D D and Le Page Y 1992 *Phys. Rev.* B **46** 5933
[84] Della Valle R J and Venuti E 1996 *Phys. Rev.* B **54** 3809
[85] Lacks D J 1998 *Phys. Rev. Lett.* **80** 5385
[86] Lacks D J 2000 *Phys. Rev. Lett.* **84** 4629
[87] Demiralp E, Cagin T and Goddard W A III 1999 *Phys. Rev. Lett.* **82** 1708
[88] Tkachenko K and Dove M T 2002 *J. Phys.: Condens. Matter* **14** 7449
[89] Gromnitskaya E L, Stal'gorova O V, Brazhkin V V and Lyapin A G 2001 *Phys. Rev.* B **64** 94205
[90] Lyapin A G, Stal'gorova O V, Gromnitskaya E L and Brazhkin V V 2002 *Zh. Eksp. Teor. Fiz.* **121** 335 (Engl. transl. 2002 *JETP* **94** 283)
[91] Lyapin A G, Brazhkin V V, Gromnitskaya E L, Mukhamadiarov V V, Stal'gorova O V and Tsiok O B 2002 *New Kinds of Phase Transitions: Transformations in Disordered Substances* ed V V Brazhkin, S V Buldyrev, V N Ryzhov and H E Stanley (Dordrecht: Kluwer) p 449
[92] Schober H, Koza M, Tölle A, Fujara F, Angell C A and Böhmer R 1998 *Physica* B **241–243** 897
[93] Rapoport E 1967 *J. Chem. Phys.* **46** 2891
Rapoport E 1968 *J. Chem. Phys.* **48** 1433
[94] Aptecar I L 1979 *Sov. Phys.–Dokl.* **24** 993
[95] Ubbelohde A 1978 *The Molten State of Matter* (New York: Wiley)
[96] Brazhkin V V 1990 *J. Non-Cryst. Solids* **124** 34
[97] Brazhkin V V, Voloshin R N, Popova S V and Umnov A G 1992 *J. Phys.: Condens. Matter* **4** 1419
[98] Tanaka H 2000 *Phys. Rev.* E **62** 6968
[99] Ryzhov V N 1990 *J. Phys.: Condens. Matter* **2** 5855
[100] Ryzhov V N and Stishov S M 2003 *Phys. Rev.* E **67** 010201(R)
[101] Brazhkin V V, Lyapin A G and Tsiok O B 1998 *Rev. High Pressure Sci. Technol.* **7** 347
[102] Huang M-Z, Ouyang L and Ching W Y 1999 *Phys. Rev.* B **59** 3540
[103] Elliot S R 1990 *Physics of Amorphous Materials* (New York: Wiley)
[104] Kelires P C 1993 *Phys. Rev.* B **47** 1829
[105] Kelires P C 1994 *Phys. Rev. Lett.* **73** 2460
[106] Kelires P C 2000 *Phys. Rev.* B **62** 15686
[107] Vitek V and Egami T 1987 *Phys. Status Solidi* b **144** 145
[108] Mishima O and Suzuki Y 2002 *Nature* **419** 599
[109] Mishima O 2000 *Phys. Rev. Lett.* **85** 334
[110] Jagla E A 2001 *Phys. Rev.* E **63** 61509
[111] Karpov V G and Oxtoby D W 1996 *Phys. Rev.* B **54** 9734
[112] Tkachenko K and Dove M T 2002 *J. Phys.: Condens. Matter* **14** 1143
[113] Guillot B and Guissani Y 1997 *Phys. Rev. Lett.* **78** 2401
[114] Agladze N I and Sievers A J 1998 *Phys. Rev. Lett.* **80** 4209
[115] Durandurdu M and Drabold D A 2001 *Phys. Rev.* B **64** 014101

[116] Mishima O and Stanley H E 1998 *Nature* **392** 164
[117] Poe B T 1997 *Annual Report* Bayreuth University p 50
[118] Brazhkin V V, Lyapin A G, Popova S V and Voloshin R N 2002 *New Kinds of Phase Transitions: Transformations in Disordered Substances* ed V V Brazhkin, S V Buldyrev, V N Ryzhov and H E Stanley (Dordrecht: Kluwer) p 15